

See discussions, stats, and author profiles for this publication at: <https://www.researchgate.net/publication/6147414>

# Insights into the Solution Structure of Human Deoxyhemoglobin in the Absence and Presence of an Allosteric Effector †

ARTICLE *in* BIOCHEMISTRY · OCTOBER 2007

Impact Factor: 3.02 · DOI: 10.1021/bi700935z · Source: PubMed

CITATIONS

18

READS

28

7 AUTHORS, INCLUDING:



**Sarata Sahu**

University of Georgia

13 PUBLICATIONS 167 CITATIONS

SEE PROFILE



**Virgil Simplaceanu**

Carnegie Mellon University

91 PUBLICATIONS 1,607 CITATIONS

SEE PROFILE



**Qingguo Gong**

University of Science and Technology of China

31 PUBLICATIONS 238 CITATIONS

SEE PROFILE



**Chien Ho**

Carnegie Mellon University

377 PUBLICATIONS 9,305 CITATIONS

SEE PROFILE

Published in final edited form as:

*Biochemistry*. 2007 September 4; 46(35): 9973–9980. doi:10.1021/bi700935z.

## Insights into the Solution Structure of Human Deoxyhemoglobin in Absence and Presence of an Allosteric Effector

Sarata C. Sahu, Virgil Simplaceanu, Qingguo Gong<sup>◇</sup>, Nancy T. Ho, Fang Tian<sup>#</sup>, James H. Prestegard<sup>#</sup>, and Chien Ho<sup>\*</sup>

Department of Biological Sciences, Carnegie Mellon University, Pittsburgh, Pennsylvania 15213, and Complex Carbohydrate Research Center, University of Georgia, Athens, Georgia 30602

### Abstract

We present a nuclear magnetic resonance (NMR) study in solution of the structures of human normal hemoglobin (Hb A) in the deoxy or unligated form in the absence and presence of an allosteric effector, inositol hexaphosphate (IHP), using <sup>15</sup>N-<sup>1</sup>H residual dipolar coupling (RDC) measurements. There are several published crystal structures for deoxyhemoglobin A (deoxy-Hb A), and it has been reported that the functional properties of Hb A in single crystals are different from those in solution. Carbonmonoxyhemoglobin A (HbCO A) can also be crystallized in several structures. Our recent RDC studies of HbCO A in the absence and presence of IHP have shown that the solution structure of this Hb molecule is distinctly different from its classical crystal structures (R and R2). In order to have a better understanding of the structure-function relationship of Hb A under physiological conditions, we need to evaluate its structures in both ligated and unligated states in solution. Here, the intrinsic paramagnetic property of deoxy-Hb A has been exploited for the measurement of RDCs using the magnetic-field dependence of the apparent one-bond <sup>1</sup>H-<sup>15</sup>N J-couplings. Our RDC analysis suggests that the quaternary and tertiary structures of deoxy-Hb A in solution differ from its recently determined high-resolution crystal structures. Upon binding of IHP, structural changes in deoxy-Hb A are also observed and these changes are largely within the  $\alpha_1\beta_1$  (or  $\alpha_2\beta_2$ ) dimer itself. These new structural findings allow us to gain a deeper insight into the structure-function relationship of this interesting allosteric protein.

Human normal adult hemoglobin (Hb A), a heterotetrameric protein that transports oxygen from the lungs to tissues, has served as an excellent model for investigating the structure-function relationship in multimeric, allosteric proteins. Hb A consists of four subunits, i.e., two identical  $\alpha$ -chains of 141 amino acid residues each and two identical  $\beta$ -chains of 146 amino acid residues each; each subunit contains a heme group leading to a complex with a molecular weight of ~ 64.5 kDa. The heme iron atom undergoes a spin-state change in going from a high-spin paramagnetic Fe<sup>+2</sup> (S=2) in the deoxy or unligated form to a diamagnetic Fe<sup>+2</sup> (S=0) in the ligated form (with O<sub>2</sub> or CO). The oxygenation of Hb A is regulated by interactions between the O<sub>2</sub>-binding sites (homotropic interactions) and interactions between individual amino acid residues in the protein molecule and various solutes (heterotropic interactions). Heterotropic effectors include hydrogen ions, chloride ions, carbon dioxide, inorganic phosphate ions, and organic phosphate ions [e.g., 2,3-bisphosphoglycerate (2,3-BPG) and inositol hexaphosphate (IHP)] and are known to modulate the oxygen affinity of hemoglobin. For reviews on the

\*Address all correspondence to Dr. Chien Ho, Department of Biological Sciences, Carnegie Mellon University, 4400 Fifth Avenue, Pittsburgh, PA 15213; telephone number: 412-268-3395; FAX number: 412-268-7083; E-mail: chienho@andrew.cmu.edu.

<sup>◇</sup>Present address: Department of Structural Biology, School of Medicine, University of Pittsburgh, Pittsburgh, PA 15261.

<sup>#</sup>University of Georgia.

<sup>†</sup>This work is supported by research grants from the National Institute of Health (R01HL-024525 and S10RR-017815 to CH and P41GM066340 to JHP).

structure-function relationship on hemoglobin, see (1–3). Allosteric effectors, 2,3-BPG and IHP, exert a significant effect on the oxygen-binding properties of Hb A. Arnone (4) reported that 2,3-BPG binds to the central cavity of the Hb molecule in the deoxy form, specifically to  $\beta$ Val1,  $\beta$ His2,  $\beta$ Lys82, and  $\beta$ His143, and thus stabilizes the deoxy quaternary structure and lowers the oxygen affinity. Arnone and Perutz (5) reported that IHP also binds to the central cavity of the deoxy-Hb A molecule, specifically at amino residues  $\beta$ His2,  $\beta$ Lys82,  $\beta$ Asp139, and  $\beta$ His143. According to Arnone and coworkers (6), IHP is disordered in the low-salt quaternary-T crystals and therefore they have not modeled the IHP molecule in its  $\beta$ - $\beta$  binding site. Yonetani et al. (7) reported that allosteric effectors, such as 2,3-BPG, bezafibrate (BZF), and IHP, affect the ligation-linked tertiary structural changes rather than the homotropic ligation-linked T/R quaternary structural transition. Recently, we have reported that IHP alters both the tertiary and the quaternary structures of HbCO A (8). It appears that the role of allosteric effectors in the structure-function relationship of Hb A is not fully understood.

Our current understanding of hemoglobin function rests largely on the crystallographic structures of ligated and unligated hemoglobin proposed by Perutz and coworkers (9,10) who identified two quaternary conformations of this protein, commonly known as the R and T states of the Monod-Wyman-Changeux (MWC) model of cooperativity (11). In the simplest description of this model, the protein switches between a tense (T), low affinity state in the unligated form, and a relaxed (R), high affinity state upon ligand binding. A new quaternary structure in the ligated state, R2, was observed by Silva et al. (12). By a comparison of the geometric coordinates of the T, R, and R2 structures, Srinivasan and Rose (13) concluded that in the transition from the unligated deoxy form to the ligated form, the quaternary structure shifts from T to R and then to R2, i.e., R is the intermediate state (13). More recently, two additional X-ray crystal structures termed R3 and RR2 have been found in the family of ligated Hb A structures by Safo and Abraham (14). Thus, HbCO A exhibits a large number of R-type crystal structures, differing in structural detail, depending on a number of factors including the crystallization conditions. There are also several X-ray crystallographic structures for deoxy-Hb A available in the Protein Data Bank [PDB accession numbers: 1A3N (15), 4HHB (16), 1HGA (17), 1KD2 (18), 1RQ3 (19), 1XXT (6), 1BZ0 (20), 1YHR (6), and 2DN2 (21)], which were crystallized under different temperature, pH, buffer, and salt conditions.

A basic assumption in correlating protein structure and function is that the structure of a protein in the crystalline state is the same as that under physiological solution conditions. It has been assumed that the weak intermolecular forces in a highly hydrated crystal are unlikely to shift the elements of a well-ordered protein relative to another one. However, this does not necessarily hold true for proteins that can switch between different conformations under allosteric control. The presence of such plasticity can be frozen out in the crystalline state; this can be even more severe for the cryo-cooled protein crystals where the structures of the highest resolution are determined. It has also been reported that the functional properties of Hb A in crystals are different from those in solution, e.g., absence of Bohr effect, cooperativity, and allosteric effector effect in the Hb crystals (22). Since the protein performs its physiological functions in the solution state, it is important as well as essential to investigate the structures of Hb A in solution, both in presence and absence of ligands and to compare them to the crystal structures. At present, there is no reported structure of deoxy-Hb A under solution conditions.

Our recent NMR structural studies using  $^{15}\text{N}$ - $^1\text{H}$  residual dipolar coupling (RDC) measurements have shown that the solution structure of HbCO A is distinctly different from the classical crystal structures (R and R2) for HbCO A. In fact, it is a dynamic ensemble between the R and R2 structures (8,23). The difference in structure between the R and R2 states is comparable in magnitude to that between the T and R states (12,24), with R2 being the farthest away from the T structure (8,13). For deoxy-Hb A, two distinct conformations with different affinity in the T state have been reported by trapping the conformations using silicate

sol-gels (25,26). This has led to speculations about the possible implications of the structural differences in the T-state of deoxy-Hb A. Thus, we need to investigate the solution structure of deoxy-Hb A and we would like to know if and what structural changes are induced by allosteric effectors.

To address these questions, we have carried out a structure investigation of deoxy-Hb A in solution in the absence and presence of IHP using the measurements of the magnetic-field induced  $^1\text{H}$ - $^{15}\text{N}$  RDCs. It is now well established that RDCs can provide direct information on the preferred orientations of various structural elements in proteins [see reviews, (27) and (28)]. However, obtaining data under conditions where small environment-induced changes are of interest is challenging. In isotropic solution, proteins assume all possible orientations with equal probability and the direct magnetic dipolar interaction between nuclei is averaged to zero. Nonzero averages giving rise to RDCs are obtained by using liquid crystal or phage medium to partially orient proteins, but the interactions with these media can create undesirable effects (29,30). Preparation in liquid crystal media can also lead to challenges when proteins need to be protected from atmospheric oxygen, or when subtle interactions with solutes are of interest. Proteins with large anisotropic magnetic susceptibilities can orient sufficiently (typically several parts per ten thousand) at high magnetic fields without the aid of liquid crystals or phage. In the case of deoxy-Hb A, despite its symmetry, orientation can be achieved due to the large anisotropy of the paramagnetic magnetic susceptibility of the hemes in the deoxy state ( $S=2$ ) and interaction of the induced moments with high magnetic fields as described previously (31). In the present study, we have extended our initial studies of the magnetic field-induced RDCs to investigate the solution structure of deoxy-Hb A in the absence and presence of IHP. The results shed new insights into the structure-function relationship in hemoglobin in solution.

## MATERIALS AND METHODS

### Sample preparation

Two-types of chain-specifically ( $\text{U-}^2\text{H}$ ,  $^{15}\text{N}$ )-labeled HbCO A samples, namely ( $\alpha$ -chains labeled and  $\beta$ -chains unlabeled) and ( $\alpha$ -chains unlabeled and  $\beta$ -chains labeled), were prepared as described previously (32). The preparation of chain-specifically labeled Hb samples in the deoxy form is described in Sahu et al. (31,33). NMR samples consisted of oxygen-free hemoglobin at 1 mM concentration (per tetramer) in 50 mM sodium phosphate buffer at pH 7.0. For IHP binding studies, the NMR samples were the same as above, except that the samples also contained 5 mM IHP.

### NMR spectroscopy

NMR experiments were carried out on four different high-field NMR spectrometers, Bruker DRX-500 and DRX-600, Varian Inova-800 and Inova-900, operating at  $^1\text{H}$  resonance frequencies of 500, 600, 800, and 900 MHz, respectively. All spectrometers were equipped with triple resonance ( $^1\text{H}$ ,  $^{13}\text{C}$ , and  $^{15}\text{N}$ ) cryo- or room temperature probes equipped with pulsed-field gradients. The J couplings were measured in the  $^{15}\text{N}$  dimension from interleaved heteronuclear single quantum coherence (HSQC) and temperature-compensated transverse relaxation-optimized spectroscopy (TROSY) spectra (34,35). All NMR measurements, both in the absence and presence of IHP, were carried out at 35 °C. The sample stability was monitored by inspecting 1D  $^1\text{H}$  and 2D HSQC and/or TROSY spectra recorded before starting and after completing the main experiments.

### RDC Analysis

If the protein is  $^{15}\text{N}$ -labeled, each amide ( $^1\text{H}$ ,  $^{15}\text{N}$ ) group can experience an RDC:

$$^1D_{NH} = D_a \left[ (3\cos^2\theta - 1) + \frac{3}{2}R\sin^2\theta\cos 2\varphi \right] \quad (1)$$

where  $D_a$  and  $R$  are the magnitude and rhombicity of the alignment tensor, and the polar angles  $\theta$  and  $\varphi$  describe the orientation of the NH bond vector with respect to the alignment frame (36). In our case,  $D_a$ ,  $R$ , and the orientation of the alignment frame with respect to the molecule were determined by fitting Eq. (1) to a set of dipolar couplings ( $^1D_{NH}$ ) measured for amides within a known, rigid, sub-structure of the protein molecule. Fitting was done using singular value decomposition (SVD) (37) or non-linear least-squares methods. Analysis included a comparison of experimental RDCs with back-calculated RDC values as described previously (23). Both root-mean square deviation (RMSD) and chi square ( $\chi^2$ ) values have been used to characterize the quality of the fit between the experimental and back-calculated RDCs. For deoxy-Hb A in absence of IHP, the errors in the observed RDCs were calculated as described by Bax et al. (38), and have been described earlier (31). In the case of deoxy-Hb A in presence of IHP, the error estimation has been carried out by repeating the RDC measurements twice under similar conditions. We have observed that the precision of measurements is a little better in the later case than the former. In both cases, the errors in the RDCs are quite small except for very few residues and the overall quality of experimental RDCs data in the presence and absence of IHP is very similar (see Figure 1 for errors in the experimental RDCs).

## RESULTS AND DISCUSSION

The first step in the structure determination of a protein using RDCs is the backbone resonance assignment. The polypeptide backbone resonance assignments of deoxy-Hb A, required for the interpretation of the backbone RDCs, were obtained using triple-resonance TROSY-based NMR experiments applied to chain-specifically labeled Hb samples (33). Assignments of deoxy-Hb A was a challenging task for a high-molecular-weight paramagnetic protein even after the assignment of its ligated, diamagnetic counterpart (HbCO A) was already solved (39). About 20% of the signals are shifted and/or severely broadened due to the presence of high-spin  $\text{Fe}^{+2}$  in the hemes of deoxy-Hb A. The presence of the hemes produces enhanced relaxation as well as causes Fermi and/or pseudo-contact interactions with nearby amino acids residues and the atoms on the porphyrins. The apparent  $^1D_{NH}$  were determined from the  $B_0^2$  dependence of the one-bond  $^{15}\text{N}$ - $^1\text{H}$  splittings ( $^1J_{NH} + ^1D_{NH}$ ), measured for deoxy-Hb A samples at four different magnetic fields (11.7, 14.1, 19.8, and 21.1 T). The field-induced RDCs are most apparent at the highest magnetic field used (900-MHz  $^1\text{H}$  frequency or 21.1 T) as described previously (31). Table 1 summarizes the  $^1\text{H}$ - $^{15}\text{N}$  RDCs for the  $\alpha_1\beta_1$  dimer of deoxy-Hb A in the absence and presence of IHP in 50 mM sodium phosphate buffer at pH 7.0 and 35 °C. The reported RDCs are taken from measurements obtained at 21.1 T.

The peaks in HSQC and TROSY spectra of deoxy-Hb A appear to be better resolved than in the corresponding spectra of HbCO A. This is not simply the result of reduced peak widths, but is also the result of reduced crowding due to the absence of peaks in deoxy-Hb A spectra for residues whose amide NH groups are close (within ~11 Å) to the paramagnetic Fe atom of the heme. RDCs used to fit Eq. (1) are restricted to those that are well resolved in the HSQC spectrum and correspond to amino acid residues located in the  $\alpha$ -helical regions of the protein molecule. This selection, along with the missing peaks for groups close to the paramagnetic heme, results in a set of 69 RDCs for the  $\alpha\beta$  dimer, 28 in the  $\alpha$ -chain and 41 in the  $\beta$ -chain. These are sufficient in number to allow evaluation of various structural models.

All published crystal structures of Hb A exhibit  $C_2$  symmetry. It is primarily the orientation of the  $\alpha_1\beta_1$  dimer relative to the  $\alpha_2\beta_2$  dimer, i.e., the orientation of the  $C_2$  axis relative to  $\alpha_1\beta_1$  that varies between T and R states. The  $C_2$  symmetry of deoxy-Hb A in solution is indicated by a single set of NMR backbone resonances for the two  $\alpha$ - and the two  $\beta$ -chains,

respectively. The  $\alpha_1\beta_1$  backbone coordinates of the well-defined helical structure segments superimpose relatively well between different unligated, T-state structures and ligated, R-state structures (R and R2) separately. The deoxy-Hb A structure does not superimpose well with the HbCO A structure (Table 2). The RMSD values between the four-selected X-ray structures of Hb A when the well-defined helical segments are superimposed are shown in a matrix form in Table 2. We have used two recent T-state structures for deoxy-Hb A and the R and R2 structures for HbCO A. This comparison can indicate that there are subtle differences at the tertiary structure level between deoxy-Hb A and HbCO A. In other words, the tertiary structures of T and R state Hb As are slightly different. The RMSD comparisons between a few selected crystal structures (two for deoxy-Hb A and two for HbCO A) are also shown in Table 2. As our preliminary results have shown (31), the crystal structure of deoxy-Hb A, 1XXT, gives the best fit to our measured RDCs. However, the quality of the fit is still not as good as that obtained in our previous work on HbCO A. This is significant considering that HSQC and TROSY spectra with better quality and resolvability have been collected for deoxy-Hb A. For 1XXT, the  $\alpha_1\beta_1$  dimer itself produces a little better fit to the measured RDCs (RMSD=1.79 Hz) than does the full tetramer (RMSD=1.92 Hz) (see Table 4). The small difference in the quality of the fit for the dimer and tetramer of deoxy-Hb A could be due to small quaternary structure changes in the solution structure of deoxy-Hb A. However, the overall lower quality than expected, implies that some of the disagreement between measured and calculated RDCs could arise from tertiary structure changes in the  $\alpha$ - and/or  $\beta$ -chains of deoxy-Hb A in solution.

It has been reported that IHP binds to the central cavity of Hb A (5) and that the central cavity in deoxy-Hb A is larger than in HbCO A (9). Allosteric effectors are known to bind much tighter in deoxy- than in ligated-Hb (1). Also, there are reports of multiple binding sites for IHP in HbCO A (40,41). All of this could lead to more extensive tertiary structure changes in the deoxy-Hb. We describe our investigation of the structural differences observed in the presence and absence of IHP on deoxy-Hb A in following paragraphs.

Nine different X-ray crystal structures of deoxy-Hb A, with the resolution ranging from 1.25 to 2.6 Å, have been selected to compare and identify which crystal structure is closer to that in solution. Detailed information about these structure files is provided in Table 3, and the details of the RDC fit to these eight different structures are shown in Table 4. The correlation plots between the observed and calculated RDCs, both in the absence and presence of IHP, based on the crystal structures 1A3N, 4HHB, 1HGA, 1KD2, 1RQ3, 1XXT, 1BZ0, 1YHR, and 2DN2 are shown in Figure 1. The scatter in these plots is in all cases larger than the estimated experimental precision (shown by error bars in the figure), and the scatter is in general larger in the presence of IHP (blue symbols) than it is in the absence of IHP (red symbols). The fitting results are also summarized in Figure 2, where a comparison of reduced chi-square ( $\chi^2$ ) of the fit to the high-resolution X-ray crystal structures in absence and presence of IHP is presented. The reduced  $\chi^2$  is defined as the  $\chi^2$  divided by the number of degrees of freedom.

The data suggest that the solution structure of the T-state hemoglobin is slightly different from all known high-resolution crystal structures available so far. As we have mentioned earlier, out of all high-resolution deoxy-Hb A structures in the Protein Data Bank, 1XXT provides the best fit to our RDC data. This result is interesting, because the highest resolution structure (2DN2) at 1.25 Å reported by Tame's group does not provide the best fit, emphasizing the fact that the structure in solution may be different.

The deviations of data from the crystal structures are even more significant in the presence of IHP. This suggests that there is a structure change in deoxy-Hb A upon IHP binding. This is not necessarily expected given the larger central cavity in the deoxy-Hb A. However, the crystal structure of deoxy-Hb A provided in 1XXT still gives the best match to experimental data.



Then, we pose the next question, of whether the structural changes induced by IHP are at the tertiary or quaternary structural levels or may be at both. We have fitted our measured RDCs to the  $\alpha_1\beta_1$  dimer as well as to the whole tetramer using eight out of the nine crystal structures (4HHB, 1HGA, 1KD2, 1RQ3, 1XXT, 1BZ0, 1YHR, and 2DN2, see Table 4 for details). We have excluded the PDB file 1A3N because a more refined structure has been reported by the same research group (PDB: 2DN2). The values for the quality of the fit to our measured RDCs in the absence and presence of IHP with these eight high-resolution X-ray structures are summarized in Figure 3 and Table 4. The results for the  $\alpha_1\beta_1$  dimer, i.e., residues 1–287, are shown as continuous filled color, while the similar results for the entire tetramer, i.e. residues 1–574 are shown with same color with stripes. In both the dimer and the tetramer fitting results, the data for deoxy-Hb A with and without IHP are shown in blue and red colors, respectively. The differences between the reduced  $\chi^2$  values between the dimer and tetramer fitting are very small whether we are using the data in the presence or absence of IHP. However, in either of the models (dimer or tetramer), the fit is better in the absence of IHP than in the presence of IHP. This is true regardless of the crystal structure used in the comparison. This is a clear indication of a significant change at the tertiary structure level. Analysis of the changes on an amino-acid-residue specific basis using just the crystal structure 1XXT is presented in Figure 4. Here the absolute differences between the observed and the calculated RDCs when fit to Hb A using the PDB structure 1XXT for different residues both in presence and absence of IHP are shown. The RDCs of the sample containing IHP are shown in blue, whereas the IHP-free sample RDCs are in red. The residue numbers for the  $\alpha_1\beta_1$  dimer (residues 1–287) followed by  $\alpha_2\beta_2$  dimer (residues 288–574) are shown along the x-axis and the corresponding absolute differences along the y-axis. More residues in the  $\beta$ -chain undergo significant changes than in the  $\beta$ -chain indicating that more residues in the  $\beta_1$ - and  $\beta_2$ -chains undergo conformational changes upon IHP binding.

### Structure change evidenced by chemical shift perturbations

Figure 5 shows representative HSQC spectra at 14.1 T of the chain-specific labeled deoxy-Hb A samples used in this work. As one can see, the addition of IHP causes a number of cross peaks to shift, especially in the  $\beta$ -chain. The assignments of  $\beta$ -chain cross-peaks for deoxy-Hb A in presence of IHP are very straightforward (33). The assignments of cross-peaks from the  $\beta$ -chain which undergo significant change in peak position in HSQC spectra were confirmed by the use of 3D  $^{15}\text{N}$ -TROSY-NOESY spectra recorded at 35 °C and 60-ms mixing time. It appears that IHP causes shifts mostly of cross-peaks from the amino acid residues located in the  $\beta$ -chain of deoxy-Hb A. This is in contrast to our previous work on the effect of IHP on HbCO A (8), where we observed chemical shift changes distributed across both  $\alpha$ - and  $\beta$ -chains. However, the current findings of a the larger effect of IHP on the  $\beta$ -chain of deoxy-Hb A are consistent with the crystallographic results on the binding of 2,3-BPG to deoxy-Hb A reported by Arnone (4). The differences between CO and deoxy behavior may result from the tendency of the smaller central cavity in ligated-Hb to more easily propagate changes throughout the protein molecule.

### Implications of the present study for the structure-function relationship in hemoglobin

There are eight unique crystal structures of deoxy-Hb A that have been deposited in the Protein Data Bank with resolution ranging from 1.25 to 2.6 Å (see Figure 1 and Tables 3 and 4). The crystal structure for 1A3N has recently been refined and its refined structure is known as 2DN2 (21). There are several interesting questions regarding these crystal structures. Does each of them exist as a discrete structure in solution? If so, what is the relative proportion for each of these structures in solution? Does each one of them exhibit its specific functional properties? Do they interconvert among themselves and if so, what is the time scale for this process in solution? As described in this paper, the solution structure of deoxy-Hb A as measured by the RDC method appears to be different from the nine crystal structures, with the crystal structure

of 1XXT giving the best fit to our RDC data (Figure 1). Does this imply that something close to the 1XXT structure is the dominant structure for deoxy-Hb A in solution, or is the apparent structure a result of more uniform averaging of data over the representative crystal structures? With respect to the latter point, a single set of cross-peaks is observed for nearly all residues. Hence, either one structure must dominate, or exchange among structures must be fast on the NMR timescale.

We can test the viability of a model in which uniform sampling of the various X-ray structures exists by using the averaging capabilities of the program, REDCAT (42).  $\alpha_1\beta_1$  dimers from seven of the unliganded X-ray structures (excluding the mutant 1YHR) were superimposed in a manner that led to overlap of the hemes in each structure, hydrogens were added to the amide sites using standard geometries, and the combined set of new coordinates was used to find the alignment parameters that best fit a model in which each of the seven structures was populated equally. The back-calculated RDCs from this model showed an RMSD relative to experiment of 1.88 Hz. This is only slightly worse than the RMSD of the 1XXT structure and it is significantly better than the average RMSD over the set of structures, 2.07. Of course, there is no reason to expect equal sampling of the X-ray structures and it is likely that populations could be adjusted to produce a better fit.

Recently, we have carried out a Model-free based NMR dynamics studies for the polypeptide backbone amide N-H bond vectors for both the deoxy- and carbonmonoxy forms of Hb A, using  $^{15}\text{N}$ -relaxation parameters and heteronuclear nuclear Overhauser effects measured at 29 and 34 °C and at 11.7 and 14.1 Tesla (43). We have found that in both deoxy- and carbonmonoxy forms of Hb A, the amide N-H bonds of most amino acid residues are rigid on the fast time scale (ns-ps), except for the loop regions and certain helix-helix connections. The C-terminal  $\beta 146\text{His}$  has been postulated to play an important role in the allostery of Hb A. Based on X-ray crystallographic data as well as its ability to form salt bridges and H-bonds in the deoxy form (9). Our backbone dynamics data indicate that this residue is rigid in the deoxy-Hb A, but it is free from restrictions to its backbone motions in the CO form, consistent with the X-ray crystallographic findings. We have found that in the deoxy form,  $\alpha 31\text{Arg}$  and  $\beta 123\text{Thr}$ , neighbors in the intra-dimer ( $\alpha_1\beta_1$ ) interface, exhibit stiffening upon CO binding. We have also found that there is considerable flexibility in the  $\alpha_1\beta_1$  interface, e.g., B, G, and H helices and the GH corner and that several amino acid residues (e.g.,  $\beta 109\text{Val}$ ) at this interface appears to be involved in a conformational exchange process in the deoxy form. We have already reported that the solution structure of HbCO A is a dynamic ensemble of the R and R2 crystal structures (23). While additional research is needed to gain a deeper insight, there is sufficient information to suggest that a dynamic ensemble may exist in the deoxy form as well.

In conclusion, the plasticity and dynamic picture of hemoglobin is consistent with the emerging view of allostery as a change in population distribution of an ensemble of structures, rather than the equilibrium of only two discrete conformations, upon binding of ligand (6,8,23,42–45). Hence, in order to understand how hemoglobin functions as an efficient oxygen carrier in our physiological system, we need to know the structure, dynamics, and function of this protein in solution.

## Acknowledgements

We thank Drs. David H. Mailliet and Xiang-jin Song for their useful discussions and critical comments. We dedicate this paper to the memory of Dr. Jonathan A. Lukin, whose research in our laboratory in Pittsburgh formed the basis for part of the work described here.



## Abbreviations used

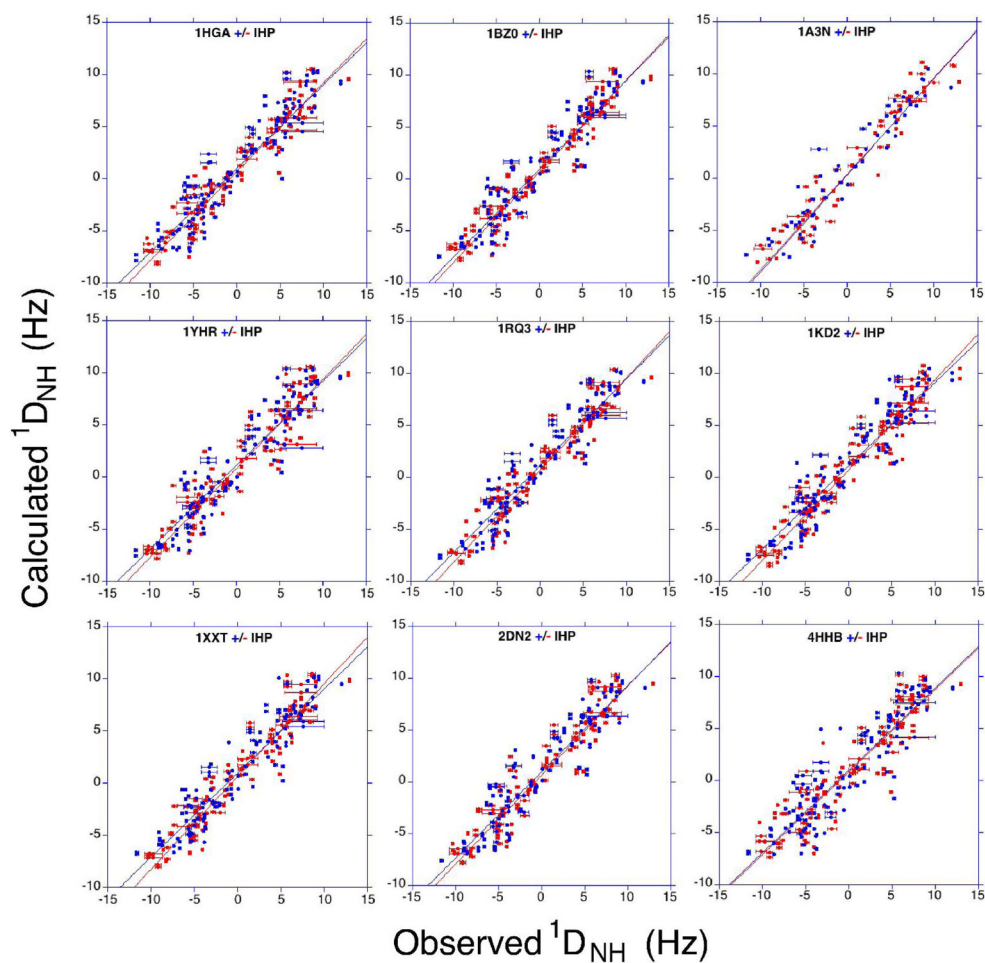
<b>Hb A</b>	human normal adult hemoglobin
<b>HbCO</b>	carbonmonoxyhemoglobin
<b>deoxy-Hb</b>	deoxyhemoglobin
<b>2,3-BPG</b>	2,3-bisphosphoglycerate
<b>IHP</b>	inositol hexaphosphate
<b>NMR</b>	nuclear magnetic resonance
<b>RDC</b>	residual dipolar coupling
<b>RMSD</b>	root-mean-square deviation
$\chi^2$	chi square
<b>HSQC</b>	heteronuclear single-quantum coherence
<b>TROSY</b>	transverse relaxation-optimized spectroscopy
<b>PDB</b>	Protein Data Bank
<b>SVD</b>	singular value decomposition

## References

1. Dickerson, RE.; Geis, I. Hemoglobin : structure, function, evolution, and pathology. Benjamin/Cummings Pub. Co.; Menlo Park, Calif: 1983.
2. Barrick D, Lukin JA, Simplaceanu V, Ho C. Nuclear magnetic resonance spectroscopy in the study of hemoglobin cooperativity. *Methods Enzymol* 2004;379:28–54. [PubMed: 15051350]
3. Lukin JA, Ho C. The structure--function relationship of hemoglobin in solution at atomic resolution. *Chem Rev* 2004;104:1219–1230. [PubMed: 15008621]
4. Arnone A. X-ray diffraction study of binding of 2,3-diphosphoglycerate to human deoxyhaemoglobin. *Nature* 1972;237:146–149. [PubMed: 4555506]
5. Arnone A, Perutz MF. Structure of inositol hexaphosphate--human deoxyhaemoglobin complex. *Nature* 1974;249:34–36. [PubMed: 4364353]
6. Kavanaugh JS, Rogers PH, Arnone A. Crystallographic evidence for a new ensemble of ligand-induced allosteric transitions in hemoglobin: the T-to-T(high) quaternary transitions. *Biochemistry* 2005;44:6101–6121. [PubMed: 15835899]

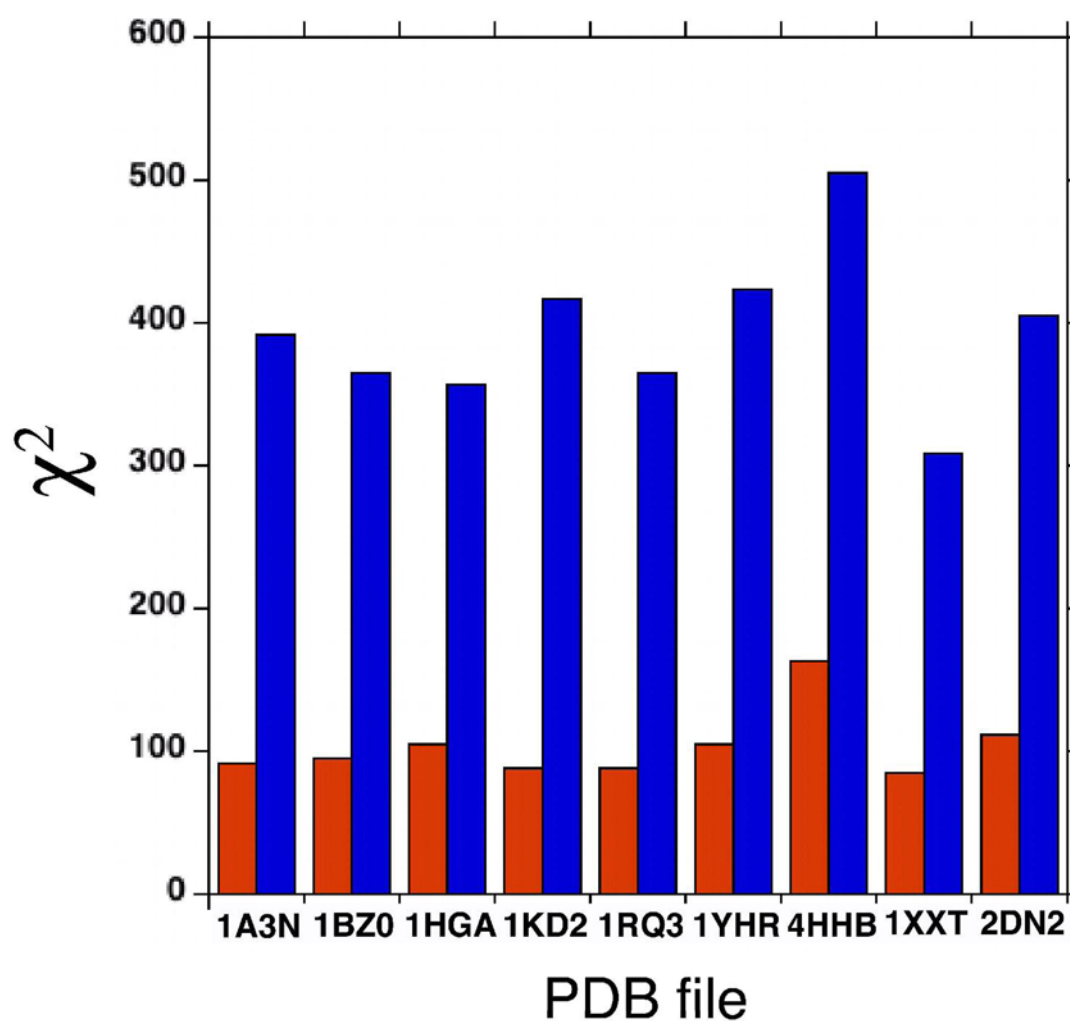
7. Yonetani T, Park SI, Tsuneshige A, Imai K, Kanaori K. Global allostery model of hemoglobin. Modulation of O(2) affinity, cooperativity, and Bohr effect by heterotropic allosteric effectors. *J Biol Chem* 2002;277:34508–34520. [PubMed: 12107163]
8. Gong Q, Simplaceanu V, Lukin JA, Giovannelli JL, Ho NT, Ho C. Quaternary structure of carbonmonoxyhemoglobins in solution: structural changes induced by the allosteric effector inositol hexaphosphate. *Biochemistry* 2006;45:5140–5148. [PubMed: 16618103]
9. Perutz MF. Stereochemistry of cooperative effects in haemoglobin. *Nature* 1970;228:726–739. [PubMed: 5528785]
10. Perutz MF, Wilkinson AJ, Paoli M, Dodson GG. The stereochemical mechanism of the cooperative effects in hemoglobin revisited. *Annu Rev Biophys and Biomol Struct* 1998;27:1–34. [PubMed: 9646860]
11. Monod J, Wyman J, Changeux JP. On the Nature of Allosteric Transitions: a Plausible Model. *J Mol Biol* 1965;12:88–118. [PubMed: 14343300]
12. Silva MM, Rogers PH, Arnone A. A third quaternary structure of human hemoglobin A at 1.7-A resolution. *J Bio Chem* 1992;267:17248–17256. [PubMed: 1512262]
13. Srinivasan R, Rose GD. The T-to-R transformation in hemoglobin: a reevaluation. *Proc Natl Acad Sci U S A* 1994;91:11113–11117. [PubMed: 7972019]
14. Safo MK, Abraham DJ. The enigma of the liganded hemoglobin end state: a novel quaternary structure of human carbonmonoxy hemoglobin. *Biochemistry* 2005;44:8347–8359. [PubMed: 15938624]
15. Tame JR, Vallone B. The structures of deoxy human haemoglobin and the mutant Hb Tyralpha42His at 120 K. *Acta Crystallogr D Biol Crystallogr* 2000;56:805–811. [PubMed: 10930827]
16. Fermi G, Perutz MF, Shaanan B, Fourme R. The crystal structure of human deoxyhaemoglobin at 1.74 Å resolution. *J Mol Biol* 1984;175:159–174. [PubMed: 6726807]
17. Liddington R, Derewenda Z, Dodson E, Hubbard R, Dodson G. High resolution crystal structures and comparisons of T-state deoxyhaemoglobin and two liganded T-state haemoglobins: T(alpha-oxy)haemoglobin and T(met)haemoglobin. *J Mol Biol* 1992;228:551–579. [PubMed: 1453464]
18. Seixas FA, de Azevedo WF Jr, Colombo MF. Crystallization and x-ray diffraction data analysis of human deoxyhaemoglobin A(0) fully stripped of any anions. *Acta Crystallogr D Biol Crystallogr* 1999;55:1914–1916. [PubMed: 10531493]
19. Chan NL, Kavanaugh JS, Rogers PH, Arnone A. Crystallographic analysis of the interaction of nitric oxide with quaternary-T human hemoglobin. *Biochemistry* 2004;43:118–132. [PubMed: 14705937]
20. Kavanaugh JS, Moo-Penn WF, Arnone A. Accommodation of insertions in helices: the mutation in hemoglobin Catonsville (Pro 37 alpha-Glu-Thr 38 alpha) generates a 3(10)→alpha bulge. *Biochemistry* 1993;32:2509–2513. [PubMed: 8448109]
21. Park SY, Yokoyama T, Shibayama N, Shiro Y, Tame JR. 1.25 Å resolution crystal structures of human haemoglobin in the oxy, deoxy and carbonmonoxy forms. *J Mol Biol* 2006;360:690–701. [PubMed: 16765986]
22. Eaton WA, Henry ER, Hofrichter J, Mozzarelli A. Is cooperative oxygen binding by hemoglobin really understood? *Nat Struct Biol* 1999;6:351–358. [PubMed: 10201404]
23. Lukin JA, Kontaxis G, Simplaceanu V, Yuan Y, Bax A, Ho C. Quaternary structure of hemoglobin in solution. *Proc Natl Acad Sci U S A* 2003;100:517–520. [PubMed: 12525687]
24. Mueser TC, Rogers PH, Arnone A. Interface sliding as illustrated by the multiple quaternary structures of liganded hemoglobin. *Biochemistry* 2000;39:15353–15364. [PubMed: 11112521]
25. Shibayama N, Saigo S. Direct observation of two distinct affinity conformations in the T state human deoxyhemoglobin. *FEBS Lett* 2001;492:50–53. [PubMed: 11248235]
26. Samuni U, Dantsker D, Juszczak LJ, Bettati S, Ronda L, Mozzarelli A, Friedman JM. Spectroscopic and functional characterization of T state hemoglobin conformations encapsulated in silica gels. *Biochemistry* 2004;43:13674–13682. [PubMed: 15504030]
27. Prestegard JH, al-Hashimi HM, Tolman JR. NMR structures of biomolecules using field oriented media and residual dipolar couplings. *Q Rev Biophys* 2000;33:371–424. [PubMed: 11233409]
28. Bax A, Grishaev A. Weak alignment NMR: a hawk-eyed view of biomolecular structure. *Curr Opin Struct Biol* 2005;15:563–570. [PubMed: 16140525]

29. Meiler J, Prompers JJ, Peti W, Griesinger C, Bruschweiler R. Model-free approach to the dynamic interpretation of residual dipolar couplings in globular proteins. *J Am Chem Soc* 2001;123:6098–6107. [PubMed: 11414844]
30. Hus JC, Peti W, Griesinger C, Bruschweiler R. Self-consistency analysis of dipolar couplings in multiple alignments of ubiquitin. *J Am Chem Soc* 2003;125:5596–5597. [PubMed: 12733874]
31. Sahu SC, Simplaceanu V, Gong Q, Ho NT, Glushka JG, Prestegard JH, Ho C. Orientation of Deoxyhemoglobin at High Magnetic Fields: Structural Insights from RDCs in Solution. *J Am Chem Soc* 2006;128:6290–6291. [PubMed: 16683773]
32. Simplaceanu V, Lukin JA, Fang TY, Zou M, Ho NT, Ho C. Chain-selective isotopic labeling for NMR studies of large multimeric proteins: application to hemoglobin. *Biophys J* 2000;79:1146–1154. [PubMed: 10920044]
33. Sahu SC, Simplaceanu V, Ho NT, Giovannelli JL, Ho C. Backbone resonance assignment of human adult hemoglobin in the deoxy form. *J Biomol NMR* 2006;36:1. [PubMed: 16703421]
34. Pervushin K, Riek R, Wider G, Wüthrich K. Attenuated T2 relaxation by mutual cancellation of dipole-dipole coupling and chemical shift anisotropy indicates an avenue to NMR structures of very large biological macromolecules in solution. *Proc Natl Acad Sci U S A* 1997;94:12366–12371. [PubMed: 9356455]
35. Kontaxis G, Clore GM, Bax A. Evaluation of cross-correlation effects and measurement of one-bond couplings in proteins with short transverse relaxation times. *J Magn Res* 2000;143:184–196.
36. Tjandra N, Bax A. Direct measurement of distances and angles in biomolecules by NMR in a dilute liquid crystalline medium. *Science* 1997;278:1111–1114. [PubMed: 9353189]
37. Losonczi JA, Andrec M, Fischer MW, Prestegard JH. Order matrix analysis of residual dipolar couplings using singular value decomposition. *J Magn Reson* 1999;138:334–342. [PubMed: 10341140]
38. Bax A, Kontaxis G, Tjandra N. Dipolar couplings in macromolecular structure determination. *Methods Enzymol* 2001;339:127–174. [PubMed: 11462810]
39. Lukin JA, Kontaxis G, Simplaceanu V, Yuan Y, Bax A, Ho C. Backbone resonance assignments of human adult hemoglobin in the carbonmonoxy form. *J Biomol NMR* 2004;28:203–204. [PubMed: 14755170]
40. Zuiderweg ER, Hamers LF, de Bruin SH, Hilbers CW. Equilibrium aspects of the binding of myo-inositol hexakisphosphate to human hemoglobin as studied by <sup>31</sup>P NMR and pH-stat techniques. *Eur J Biochem* 1981;118:85–94. [PubMed: 7285915]
41. Zuiderweg ER, Hamers LF, Rollema HS, de Bruin SH, Hilbers CW. <sup>31</sup>P NMR study of the kinetics of binding of myo-inositol hexakisphosphate to human hemoglobin. Observation of fast-exchange kinetics in high-affinity systems. *Eur J Biochem* 1981;118:95–104. [PubMed: 7285916]
42. Valafar H, Prestegard JH. REDCAT: A residual dipolar coupling analysis tool. *J Magn Res* 2004;167:228–241.
43. Song X, Yuan Y, Simplaceanu V, Sahu SC, Ho NT, Ho C. A Comparative NMR Study of the Backbone Dynamics of Hemoglobin in the Deoxy and Carbonmonoxy Forms. *Biochemistry* 2007;46:6795–6803. [PubMed: 17497935]
44. Gunasekaran K, Ma B, Nussinov R. Is allostery an intrinsic property of all dynamic proteins? *Proteins* 2004;57:433–443. [PubMed: 15382234]
45. Kern D, Zuiderweg ER. The role of dynamics in allosteric regulation. *Curr Opin Stru Biol* 2003;13:748–757.



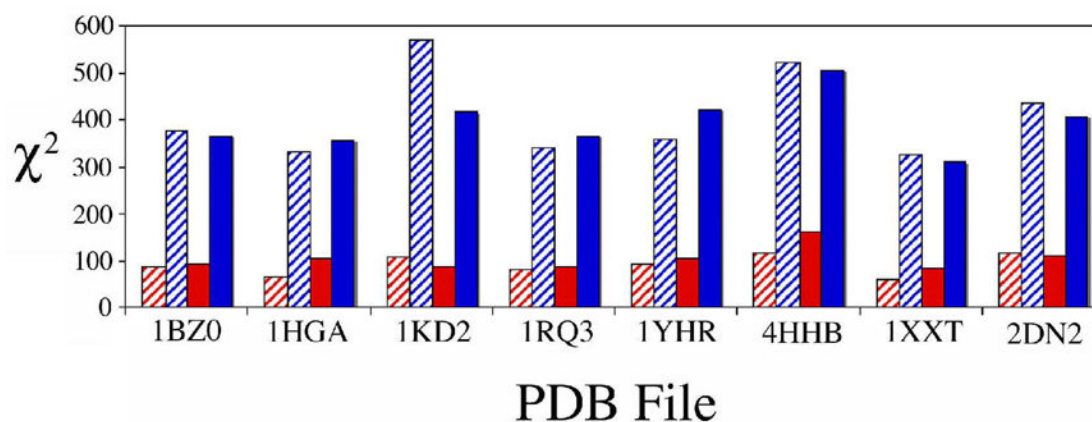
**Figure 1.**

The correlation between the observed and calculated RDC values both in the presence and absence of IHP, based on the crystal structures 1A3N, 4HHB, 1HGA, 1KD2, 1RQ3, 1XXT, 1BZ0, 1YHR, and 2DN2 for deoxy-Hb A. For details about these PDB files, see the Table 2. The data in the absence of IHP are shown in red and in the presence of IHP are shown in blue. Errors in the observed RDC are also shown and depicted in the same color as above.



**Figure 2.**

The quality of fit results from the correlation plots is shown in Figure 1. The X-ray crystal structure file names are shown along the x-axis and their corresponding reduced  $\chi^2$  values in the absence (red) and presence (blue) of IHP are along the y-axis.

**Figure 3.**

Summary of the fitting quality of our measured RDCs in the absence and presence of IHP to eight high-resolution x-ray crystal structures: 4HHB, 1HGA, 1KD2, 1RQ3, 1XXT, 1BZ0, 1YHR, and 2DN2. X-ray structure file names are shown along the x-axis and the corresponding reduced  $\chi^2$  values of the fit to either the  $\alpha_1\beta_1$  dimer (in striped symbol) only or the whole tetramer (in filled symbol) are along the y-axis, red color for the structure in the absence of IHP and blue color for the structure in the presence of IHP.



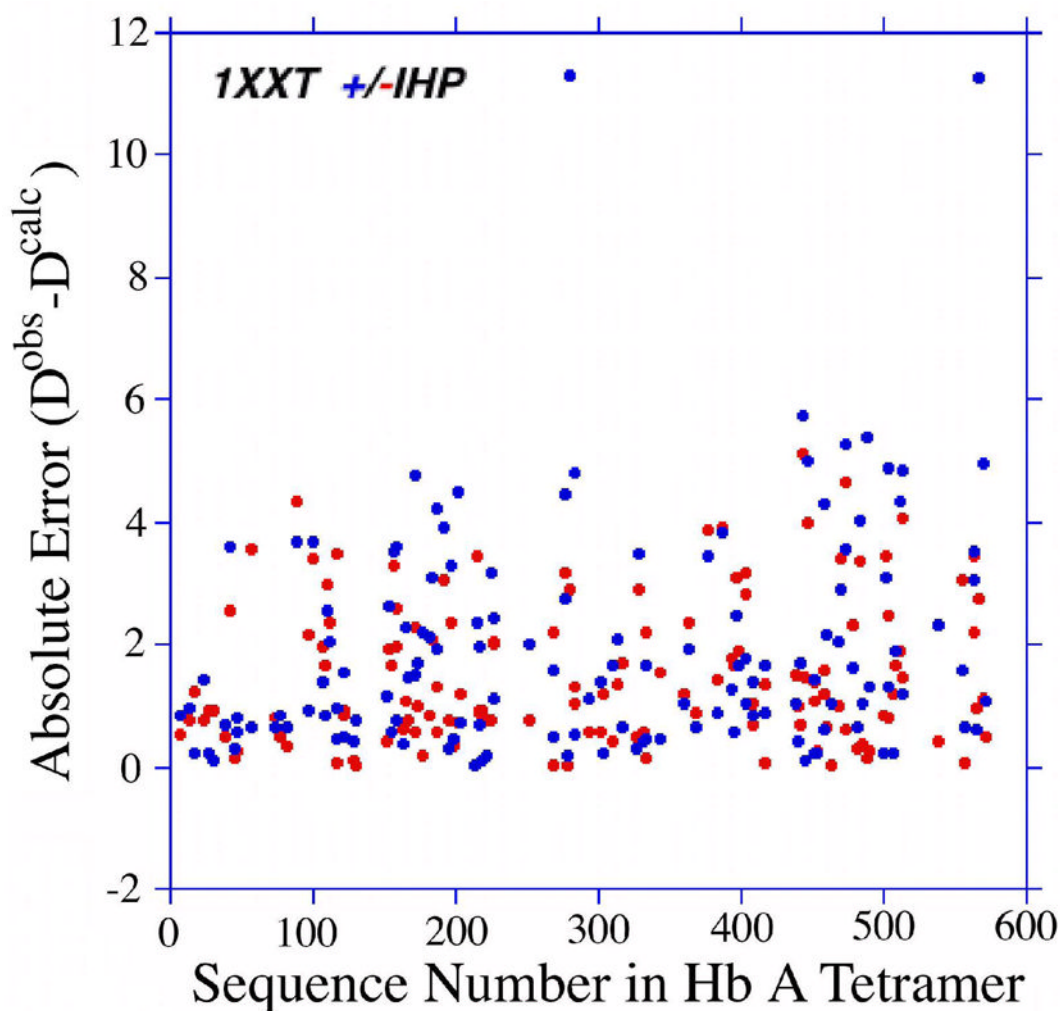


**Figure 4.**

Difference (absolute value) between the observed and the calculated RDCs when fitting to deoxy-Hb A using the PDB crystal structure 1XXT. The amino acid residue numbers for the  $\alpha_1\beta_1$  dimer (residues 1–287) followed by  $\alpha_2\beta_2$  dimer (residues 288–574) are shown along the x-axis and the corresponding absolute differences along the y-axis. RDCs of the sample containing IHP are shown in blue, whereas the IHP-free sample RDCs are in red.

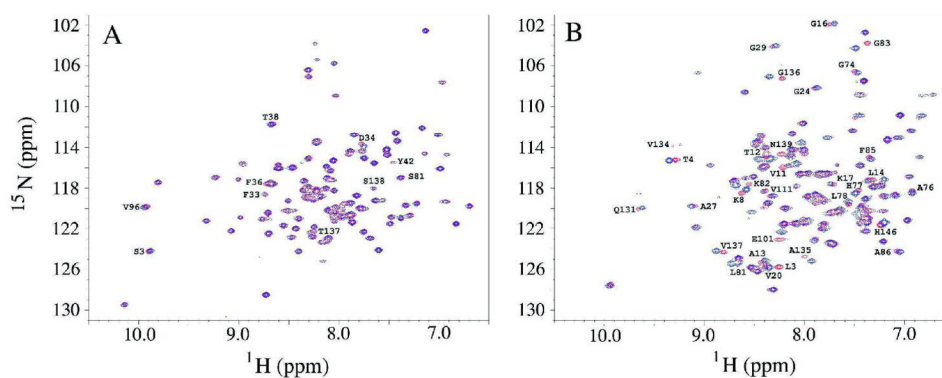


**Figure 5.** 600-MHz ( $^1\text{H}$ ,  $^{15}\text{N}$ ) HSQC spectra of chain-specifically labeled-deoxy-Hb A with IHP (blue) and without IHP (red) at 35 °C: (A) ( $\text{U-}^{15}\text{N}$ ,  $^2\text{H}$ )-labeled  $\alpha$ -chains and unlabeled  $\beta$ -chain-chains; and (B) unlabeled  $\alpha$ -chains and ( $\text{U-}^{15}\text{N}$ ,  $^2\text{H}$ )-labeled  $\beta$ -chains. In all samples, the Hb concentration was ~1 mM in 50 mM sodium phosphate at pH 7.0 and the IHP samples also contained 5 mM IHP.

**Table 1**

$^1\text{H}$ - $^{15}\text{N}$  RDC values for the  $\alpha_1\beta_1$  dimer of deoxy-Hb A in the absence and presence of IHP in 50 mM sodium phosphate buffer at pH 7.0 and 35 °C. The reported RDCs are taken from the measurements obtained at 21.1 T.

Residue No.	Residue Name	Chain ID	RDC (Hz) – IHP	RDC (Hz)+IHP
6	ASP	$\alpha_1$	-1.57±0.18	-2.84±0.11
14	TRP	$\alpha_1$	-4.71±0.31	-5.01±0.20
16	LYS	$\alpha_1$	-5.46±0.17	-5.43±0.10
23	GLU	$\alpha_1$	3.86±0.33	2.21±0.08
26	ALA	$\alpha_1$	1.66±0.24	1.78±0.16
30	GLU	$\alpha_1$	0.54±0.45	0.94±0.23
39	THR	$\alpha_1$	5.10±0.65	5.51±0.12
41	THR	$\alpha_1$	-9.72±1.03	-8.98±0.17
45	HIS	$\alpha_1$	-4.89±0.30	-5.26±0.29
46	PHE	$\alpha_1$	-5.44±0.15	-5.52±0.14
47	ASP	$\alpha_1$	-3.52±0.12	-4.03±0.10
57	GLY	$\alpha_1$	-5.68±1.21	-3.85±0.05
73	VAL	$\alpha_1$	6.63±0.13	6.49±0.07
76	MET	$\alpha_1$	-4.05±0.11	-3.79±0.06
81	SER	$\alpha_1$	0.44±0.35	0.08±0.09
89	HIS	$\alpha_1$	1.44±0.44	1.44±0.44
96	VAL	$\alpha_1$	7.30±1.87	8.02±0.14
100	LEU	$\alpha_1$	5.79±0.46	5.79±0.46
107	VAL	$\alpha_1$	8.55±0.43	8.84±0.11
108	THR	$\alpha_1$	8.70±0.24	9.37±0.11
110	ALA	$\alpha_1$	12.90±0.18	12.04±0.09
112	HIS	$\alpha_1$	6.26±0.16	5.57±0.09
116	GLU	$\alpha_1$	-10.3±0.14	-6.67±0.16
117	PHE	$\alpha_1$	-1.06±0.13	-0.56±0.07
121	VAL	$\alpha_1$	7.35±0.17	8.69±0.09
122	HIS	$\alpha_1$	7.24±0.15	5.48±0.13
129	LEU	$\alpha_1$	6.10±0.24	6.18±0.08
130	ALA	$\alpha_1$	5.80±0.22	5.63±0.15
152	VAL	$\beta_1$	4.81±0.16	4.60±0.10
153	THR	$\beta_1$	4.04±0.20	4.36±0.22
155	LEU	$\beta_1$	9.04±0.19	8.12±0.12
157	GLY	$\beta_1$	-7.29±0.30	-6.41±0.18
158	LYS	$\beta_1$	8.44±0.28	7.30±0.17
159	VAL	$\beta_1$	4.86±0.20	5.25±0.22
164	VAL	$\beta_1$	-0.77±0.23	-0.76±0.14
165	GLY	$\beta_1$	4.02±0.31	2.57±0.16
166	GLY	$\beta_1$	5.61±0.33	4.55±0.16
171	ARG	$\beta_1$	-1.20±0.41	-1.24±0.20
172	LEU	$\beta_1$	1.18±1.16	-3.24±0.89
173	LEU	$\beta_1$	7.04±2.25	7.60±2.42
176	TYR	$\beta_1$	3.97±0.43	1.85±0.36
181	ARG	$\beta_1$	-4.36±0.44	-4.03±0.25
183	PHE	$\beta_1$	-4.93±0.87	-5.31±0.94
186	PHE	$\beta_1$	7.44±0.27	3.28±0.19
187	GLY	$\beta_1$	5.72±0.11	4.78±0.09
191	THR	$\beta_1$	-3.01±0.11	-3.25±0.12
195	VAL	$\beta_1$	-3.63±0.13	-3.91±0.14
197	GLY	$\beta_1$	-2.81±0.23	-4.74±0.11
198	ASN	$\beta_1$	3.30±0.18	3.53±0.11
202	LYS	$\beta_1$	-1.44±0.22	-6.00±0.15
203	ALA	$\beta_1$	-5.25±0.30	-5.67±0.32
213	SER	$\beta_1$	-1.97±0.56	-2.12±0.61
215	GLY	$\beta_1$	-5.76±0.37	-5.93±0.17
216	LEU	$\beta_1$	0.58±0.19	-0.99±0.11
217	ALA	$\beta_1$	-8.28±0.14	-7.37±0.11
219	LEU	$\beta_1$	6.13±0.24	6.64±0.15
221	ASN	$\beta_1$	8.98±0.13	9.02±0.09
225	THR	$\beta_1$	-8.07±0.33	-9.08±0.18
226	PHE	$\beta_1$	-3.65±0.25	-3.08±0.15
227	ALA	$\beta_1$	-4.42±0.21	-4.54±0.10
252	VAL	$\beta_1$	7.78±0.27	4.73±0.24

Residue No.	Residue Name	Chain ID	RDC (Hz) – IHP	RDC (Hz)+IHP
268	GLN	$\beta_1$	$-8.59 \pm 0.19$	$-6.89 \pm 0.11$
269	ALA	$\beta_1$	$-5.10 \pm 0.19$	$-3.74 \pm 0.15$
276	ALA	$\beta_1$	$-10.1 \pm 0.60$	$-8.70 \pm 0.15$
277	GLY	$\beta_1$	$-4.85 \pm 0.27$	$-5.70 \pm 0.17$
278	VAL	$\beta_1$	$-2.81 \pm 0.27$	$-2.49 \pm 0.28$
280	ASN	$\beta_1$	$-7.70 \pm 0.26$	$-15.3 \pm 0.11$
283	ALA	$\beta_1$	$-9.16 \pm 0.32$	$-11.6 \pm 0.20$
284	HIS	$\beta_1$	$5.92 \pm 0.34$	$7.20 \pm 0.08$

**Table 2**

RMSD matrix between the structured regions in the  $\alpha_1\beta_1$  dimer of Hb A in Å units. The PDB IDs and the crystallization conditions for the T and R state structures are also given.

PDB ID → ↓	T (1XXT)	T (2DN2)	R (1IRD) (high salt)	R2 (1BBB) (low salt)
T (1XXT)	0.00	0.24	0.98	1.05
T (2DN2)	0.24	0.00	0.93	1.00
R (1IRD) (high salt)	0.98	0.93	0.00	0.37
R2 (1BBB) (low salt)	1.05	1.00	0.37	0.00

**Table 3**

Various high-resolution crystal structures of deoxy-Hb A used in our analysis. The different names in this table are the standard PDB nomenclatures.

PDB ID	Resolution (Å)	R factor	Compound	Ligation State
1A3N	1.8	0.171	HEM, ABCD	Deoxy, T
4HHB	1.74	0.135	HEM, PO <sub>4</sub> , ABCD	Deoxy, T
1HGA	2.1	0.2	HEM, ABCD	Deoxy, T
1KD2	1.87	0.198	HEM, ABCD	Deoxy, T (high affinity)
1RQ3	1.91	0.167	HEM, ABCD	Deoxy, T
1XXT	1.91	0.19	HEM, ABCD	Deoxy, T
1BZ0	1.5	0.167	HEM, ABCD	Deoxy, T
1YHR <sup>a</sup>	2.6	0.185	HEM, ABCD, O <sub>2</sub>	Oxy, T (high)
2DN2	1.25	0.179	HEM, ABCD	Deoxy, T

<sup>a</sup>Crystallized with 10 mM IHP and 20% PEG.



**Table 4**  
Fitting results obtained from the  $\alpha_1\beta_1$  dimer and the full tetramer of different deoxy-Hb A structures.

PDB ID	IHP	$\chi$ [Dimer]	$\chi^2$ [Tetramer]	RMSD (Hz) [Dimer]	RMSD (Hz) [Tetramer]	$D_a$ (Hz) [Dimer]	R [Dimer]	$D_a$ (Hz) [Tetramer]	R [Tetramer]
1BZ0	–	88.5	95.2	2.037	2.025	5.49	0.31	5.49	0.31
	+	376.4	365.0	2.631	2.607	5.29	0.32	5.39	0.28
1HGA	–	64.9	104.5	1.890	2.241	5.37	0.33	5.37	0.39
	+	332.8	357.0	2.528	2.626	5.27	0.39	5.27	0.34
1KD2	–	109.5	88.6	2.199	2.030	5.37	0.28	5.37	0.42
	+	569.5	417.2	3.190	2.672	5.27	0.13	5.37	0.35
1RQ3	–	81.7	88.3	2.042	1.969	5.37	0.42	5.37	0.39
	+	341.4	365.5	2.511	2.523	5.27	0.46	5.27	0.33
1YHR	–	92.1	104.5	2.186	2.241	5.37	0.29	5.37	0.37
	+	358.3	422.9	2.647	2.733	5.27	0.36	5.27	0.34
4HHB	–	119.6	163.0	2.286	2.458	5.43	0.29	5.22	0.28
	+	522.5	504.9	3.168	2.943	5.19	0.03	5.24	0.31
1XXT	–	61.0	85.4	1.790	1.923	5.37	0.39	5.37	0.38
	+	325.2	309.0	2.404	2.659	5.27	0.37	5.27	0.21
2DN2	–	119.7	112.2	2.272	2.196	5.32	0.40	5.37	0.34
	+	435.0	405.6	2.732	2.704	5.12	0.37	5.27	0.33